Dynamic data collection algorithm based on mobile edge computing in underwater internet of things

Xiaoyun Guang, Chunfeng Liu*, Wenyu Qu and Zhao Zhao

Abstract

The Underwater Internet of Things (UIoT) has emerged as one of the prominent technologies in the development of future ocean monitoring systems, where mobile edge elements (such as autonomous underwater vehicles (AUVs)) provide a promising method for the data collection from sensor nodes. However, as an important part of the UIoT, underwater wireless sensor networks (UWSNs) are severely affected by the underwater dynamic environment. For instance, node locations change continuously, which significantly increases the difficulty of data collection. To solve this problem, the concept of an inevitable communication space (ICS) is proposed. The ICS is calculated by analyzing the variation in the position of nodes and the communication range. Furthermore, an ICS-based dynamic data collection algorithm (ICS-DDCA) for UIoT is proposed to collect underwater data. This method utilizes the ICS instead of the initial location of the node for data collection to further improve the performance of the algorithm and shorten the data collection time. The simulation results demonstrate that compared with the energy-efficient data collection over AUV-assisted (EEDA) and data collection algorithms based on probabilistic neighborhood (PNCS-GHA), ICS-DDCA can effectively reduce the collection time, while ensuring the full completion of data collection.

Keywords UIoT, Underwater wireless sensor networks, Data collection, AUV, Path planning, Mobile node

Introduction

The Internet of Things (IoT) has widely applied in smart home, smart city, and transportation [1–4]. As the important technologies of the IoT, mobile devices and wireless technologies provide great potential developments for mobile edge computing [5]. Mobile edge computing is a computing paradigm that implements cloud computing services on the edges of network by using mobile edge devices. Mobile edge devices are closer to the network edge and have the advantages of storage, mobility, and computing.

As an extension of IoT in the marine environment, Underwater Internet of Things (UIoT) has a wide application prospect in water quality monitoring, pollution observation, ocean resource exploration [6], which have attracted more and more attention from academic institution and industry [7, 8]. Underwater wireless sensor network (UWSN) is an imprtant part of the UIoT, which is composed of a large number of underwater sensor nodes (i.e., anchored nodes, mobile nodes, and surface sink) with the ability to sensing, acquisition and communication [9]. Underwater node can communicate with other node via underwater acoustic links. In most of UIoT, underwater sensor nodes are fixed by anchor rope to prevent them from being washed away by the current. Anchored sensor nodes towed by rope move within a certain range with the water current and perceive data of the surrounding environment. Then the perceived data is collected to the sink node on water surface or base station on near shore for further process. Data collection in the UIoT can be regarded as a mobile edge application [10].

*Correspondence:
Chunfeng Liu
cfliu@tju.edu.cn
College of Intelligence and Computing, Tianjin University, Tianjin, China

Guang *et al. Journal of Cloud Computing*   (2023) 12:46

Page 2 of 14

Multi-hop data collection methods and autonomous underwater vehicle aided (AUV-aided) data collection methods are common methods for data collection [11, 12]. The advantage of the former is that the data collection delay is shorter than using AUV to collect data. However, the drawback of multi-hop data collection is that nodes have the problem of unbalanced energy consumption [13, 14]. The forwarding nodes close to the sink node consume more energy [15]. Besides, the mobility of nodes leads to dynamic changes in the network topology and even leads to communication interruption, thus affecting the feasibility of the multi-hop data collection algorithms. The latter can compensate for the defect of unbalanced energy consumption caused by multi-hop transmission [16–18] and be more tolerant to frequent topology changes. However, in the dynamic underwater environment, the actual position of the anchored node does not always stay at its initial position because of the anchored node moves within a certain range with the water current. When AUV moves to the predefined position according to a certain strategy, the nodes may have deviated from their initial position, hindering data collection. In order to successfully collect the data perceived by anchored nodes, AUV needs to move with the node. The time of data collection is largely prolonged. This study aims to resolve the problem by eliminating the side effects caused by the mobility of nodes to reduce the path length of AUV and the time of data collection.

To address this problem, a new concept of inevitable communication space (ICS) based on communication range and movement range of node is proposed. By calculating the ICS, AUV does not need to consider the exact position of sensor node any more for data collection. As long as AUV passes through the ICS of sensor node, it is ensured to have a link between AUV and this node to communicate with each other. Furthermore, an ICS-based dynamic data collection algorithm (ICS-DDCA) is proposed to reduce the path length of AUV, where the ICS information is used instead of the initial position of the anchored nodes to plan the route of data collection for AUV.

To the best of our knowledge, using the ICS to eliminate the impact of node mobility is a highly efficient method for path planning of AUV. The main contributions of this study are as follows:

1. The concept of inevitable communication space (ICS) based on node mobility is proposed. The ICS is calculated by analyzing the variation in the position of nodes and the communication range while fully considering the mobility of nodes.
2. An ICS-based dynamic data collection algorithm (ICS-DDCA) is proposed, which makes AUV pass through the ICS instead of the initial position, thereby shortening the path length.

The remainder of this paper is organized as follows. In Section 2, a brief survey of underwater data collection is presented. Section 3 describes the network model of UIoT. Section 4 analyzes the theoretical basis of ICS and presents the calculation steps. Section 5 proposes an ICS-based dynamic data collection algorithm. The experimental results are presented in Section 6. Finally, in Section 7, the main results are summarized, and future research is discussed.

Related works

Researchers have proposed numerous data collection methods for UIoT. Some works are listed in Table 1.

In the multi-hop data collection scheme, nodes transmit data to the sink node through a multi-hop process of underwater acoustic communication. A typical multi-hop collection method is depth-based routing protocol (DBR) [19]. DBR transmits data to sink node along the

Table 1 Comparison of data collection methods

Data collection methods	Algorithms	Research contributions	Shortcomings
Multi-hop data collection	DBR [19]	Reducing energy consumption and collision	Energy imbalance
	EECOR [20]	Alleviating packet collisions	Energy imbalance
	RMER [21]	Reducing energy consumption	Multipath interference
	EELA [22]	Improving positioning accuracy	Energy imbalance
AUV-aided data collection	Mobicast [17], GAAP [18], PNCS-GHA [23]	Collecting data effectively	Large delay
	EEDA [24]	Balancing energy consumption	Suitable for dense networks
	PPM-LUWSN [25]	Shortening the mobile path while ensuring data collection	Suitable for 2D space
	SDCS [26]	Reducing energy consumption and balancing the energy consumption	Some edge nodes may lose packets due to movement

Guang *et al. Journal of Cloud Computing*   (2023) 12:46

Page 3 of 14

direction of depth reduction. Because the depth information of nodes are more accessible, DBR replaces the location information with depth information of nodes. To address the energy-limitation problem, either the best relay nodes are selected or a periodic sleep/activation mode is used to reduce energy consumption [20, 21]. In a sparse network, the routing overhead of data collection can be reduced via power adjustments. Yuan et al. utilized a single-leader-multi-follower Stackelberg game to propose the Energy-Efficient Localization Algorithm (EELA) to adjust the communication power [22]. Even great efforts have been tried, unbalanced energy consumption is still a non-negligible problem in multi-hop data collection scheme.

To solve the unbalanced energy consumption problem, some studies [17, 18, 23, 27] used AUVs or mobile nodes to collect underwater data. Chen et al. [17] proposed the Mobicast method for static sensor nodes, where AUV collects data according to the user-defined paths. Gjanci et al. [18] designed a greedy and adaptive AUV path-finding (GAAP) heuristic algorithm to prioritize data collection with different information value. Han et al. [23] proposed a data collection algorithms based on probabilistic neighborhood for underwater acoustic sensor networks (PNCS-GHA), in which the AUV traverses a probabilistic neighborhood covering set for data collection. Gao et al. [27] proposed that the target nodes in the monitoring area can be covered by multiple AUVs or multiple mobile nodes to complete the data collection. To balance the energy consumption of the nodes, Yan et al. [24] proposed the energy-efficient data collection over AUV-assisted (EEDA), in which the network is divided into several small areas according to the deployment of data receivers. The sensor nodes relay data to a data receiver through a rigid graph, and AUV traverses the data receivers to retrieve the data. In [10, 28], it is assumed that the network is clustered with cluster heads and ordinary nodes. The ordinary node sends data to its cluster head, and AUV visits all the cluster heads to collect data. The energy consumption is balanced by regularly updating cluster heads. Cheng et al. [29] proposed a data gathering protocol that considers the importance of data. Important data are transmitted to the sink node through multi-hop routing. Other nodes forward the data to nodes close to AUV. Then, these nodes transmit the data directly to AUV.

Considering node mobility, Zhou et al. [25] proposed a path planning method based on the location uncertainty of water surface nodes (PPM-LUWSN) to collect data. In this structure, multiple anchored nodes are fixed at different depths via an anchor rope, and the anchor nodes located on the same rope transmit data to the

water surface nodes through multi-hop transmission. Then, a high-altitude unmanned aerial vehicle (UAV) visits the water surface nodes to collect the stored data, which are restricted mobile nodes. The deviation range of the water surface node is limited to a circle, thus, this method is suitable for 2D structures in special environments. In a 3D underwater space, the movement of the nodes is more complex. The deviation range of the nodes is no longer limited to a circle, but a 3D space. Considering the characteristics of water delamination, Han et al. [26] divided the network into two layers with different mobility characteristics, and proposed a stratification-based data collection scheme (SDCS). The nodes in the upper layer move with the water flow, and transmit data through a multi-hop process. The nodes in the lower layer are considered as relatively static, and AUV is used to collect data in this layer. By using different data collection algorithms in different network layers, the energy consumption of nodes can be reduced and the network lifetime can be prolonged. However, this method is suitable for the specific underwater environment.

In summary, the existing data collection methods rarely consider the data collection problem due to node movement in a 3D underwater space. For a 3D dynamic underwater environment, the sensor node may have moved to other locations before AUV arrives at the pointed location according to the planned path. Therefore, it increases the difficulty of data collection and prolongs the time of data collection. Thus, static location-based path planning of AUV is not adequate for effective data collection. Therefore, considering the mobility of nodes in 3D underwater environment, a dynamic data collection algorithm is proposed in this paper. This article attempts to reduce the time of data collection and improve the efficiency of data collection.

Network model
Model description
We investigate the problem in a 3D underwater space with a monitoring area of $L \times W \times H$, where L, W, and H are length, width, and depth respectively. The monitoring area is described by a 3D coordinate system with coordinate axes, as illustrated in Fig. 1. The UIoT consists of N underwater anchored nodes, capable of sensing data from surrounding environment, and AUV can move around and be responsible for collecting the data sensed by underwater anchored nodes. The set of anchored nodes is $V = \{V_1, V_2, \ldots, V_N\}$. The anchored sensor nodes are prone to deviate from their initial position and move within a spherical crown surface due to the influence of water flow [30, 31].
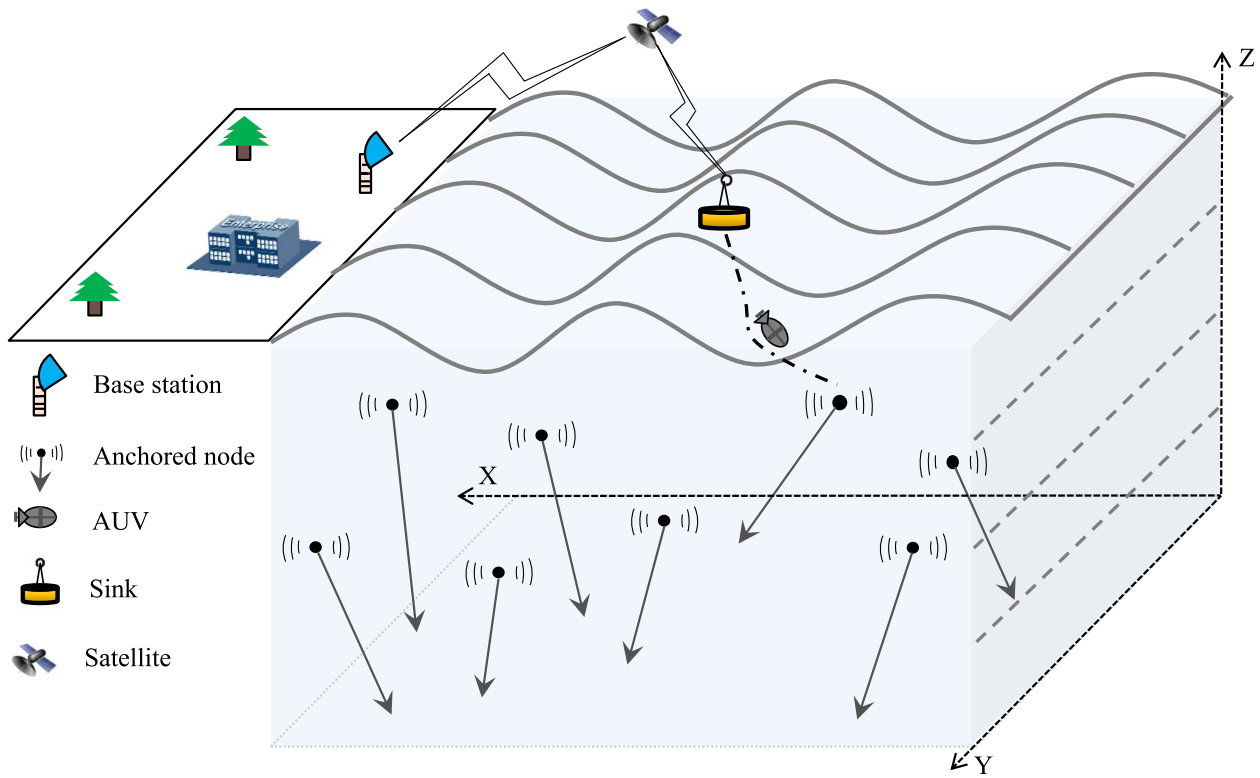
Guang *et al. Journal of Cloud Computing* (2023) 12:46

Page 4 of 14

Fig. 1 Network architecture

For $\forall V_k \in V$, its communication radius and deviation radius at time t are denoted as $Rc(k)$ and $Ra(k)^t$. As shown in Fig. 2, θ is the maximum offset angle, ϕ_k^t is the current offset angle with respect to the initial position of node V_k, and l_k is the length of anchor rope of node V_k. The deviation radius at time t can be calculated by l_k and ϕ_k^t, that is $Ra(k)^t = l_k \sin \phi_k^t$ [30]. During the offset movement, the possible locations of anchored node V_k shape a spherical crown SC_k. The node coordinates regarding the initial and offset positions at time t are denoted as (x_k^0, y_k^0, l_k) and (x_k^t, y_k^t, z_k^t), respectively. Consequently, based on the initial position and offset angle, the coordinate of V_k at time t can be expressed as [30, 31]

$$\begin{cases} x_k^t = x_k^0 + l_k \sin \phi_k^t \cos \phi_k^{'t} \\ y_k^t = y_k^0 + l_k \sin \phi_k^t \sin \phi_k^{'t} \\ z_k^t = |l_k \cos \phi_k^t| \end{cases} \quad (1)$$

where $\phi_k^t \in (0, \theta]$, $\phi_k^{'t}$ is the angle between the projection of the anchored rope in the x-y plane and the x-axis. The distance between the initial position and current position of node is $\sqrt{(x_k^t - x_k^0)^2 + (y_k^t - y_k^0)^2 + (z_k^t - l_k)^2} = l_k \sqrt{2(1 - \cos \phi_k^t)}$. When the length of the anchor rope is fixed, the larger the offsetting angel is, the longer the distance of node motion will be. The offset angle determines whether the

node is still in the initial communication range after movement.

The offset angle is related to the movement of the current model. According to the typical multi-layer current model [32], the network monitoring area is divided into several layers. The ocean currents move at a constant speed and direction within a certain layer. The speed and direction of ocean currents affect the offset angle. In a more realistic scenario, a layer with greater depth has a smaller current velocity [33]. The nearer a layer is to the water surface, the greater the water flow rate is.

Definitions and assumptions

Homogeneous anchored sensor nodes are considered in this paper. All anchored sensor nodes are assumed to have the same capability of computing, sensing, and communication. To clarify the network model and simplify the problem, other assumptions and definitions are provided.

Assumptions:

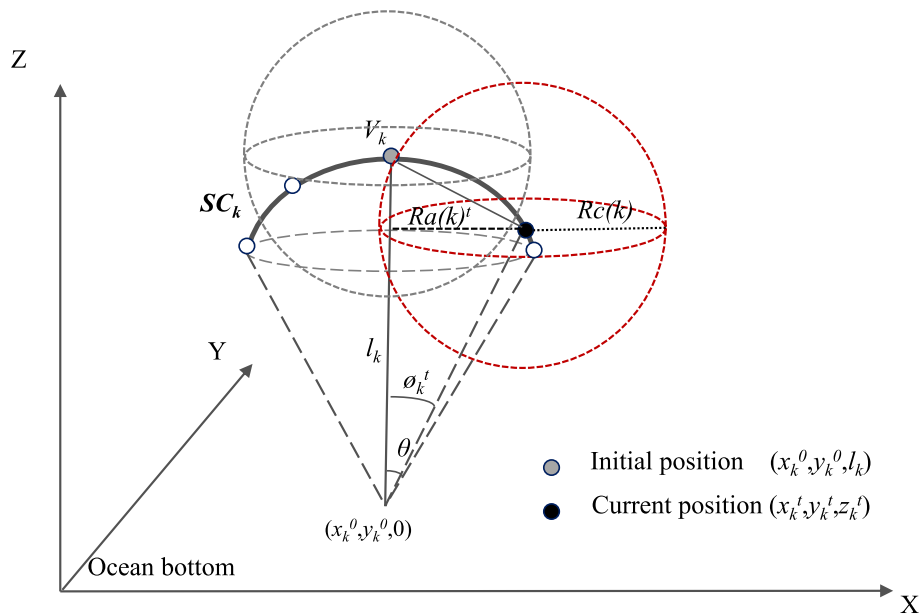1 The anchor nodes are randomly deployed in the 3D underwater environment.

Fig. 2 Model of node movement

2 The initial locations of anchored nodes are known (e.g., from manual deployment or by using localization techniques), but the locations after movement are unknown.

3 $Ra_m(k) < Rc(k)$, $Ra_m(k)$ is the maximum deviation radius corresponding to the maximum offset angle θ.

4 The velocity of AUV is constant and set to v_m.

Definition 1: Inevitable communication space (ICS) of node. For $\forall V_k \in V$, the ICS of V_k is defined as $\text{ICS}(V_k, Rc(k)) = \cap_{\forall p_k \in SC_k}\{q \mid d(p_k, q) \le Rc(k)\}$, where q is a point in UIoT and p_k is a point in SC_k.

Calculation of ICS

Owing to the influence of water flow, the anchored nodes are likely to drift off their initial positions. Furthermore, their deviation range is a spherical crown surface, as shown in Fig. 2. The red dotted sphere represents the possible communication range when the node is at the current deviation position. The offset movement of nodes within the spherical crown surface results in an uncertain node position. The location uncertainty increases the difficulty of underwater data collection. To reduce the time and difficulty of collecting data while considering the node offset movement, the ICS of nodes is calculated, which is the intersection of all possible communication ranges.

When the communication radius is larger than the maximum deviation radius, the ICS of nodes exists. Regardless of where the node is within its deviation

range, AUV can communicate with the sensor node granted it passes through the ICS.

Calculating the ICS of a node is crucial. The calculation steps of the ICS are as follows:

Step 1. According to the sampling segmentation method, the offset angle is evenly divided into several equal angles. Then, we cut the spherical crown surface into several circles with decreasing radii, as shown in Fig. 3(a). The anchored node can be seen as moving on the circles whose center is on a straight line but whose radius varies. The circles are called deviation circles. A 3D spherical communication range exists at each possible location, as shown in Fig. 3(a). In Fig. 3(a), O_1 and O_2 are the boundary locations where node V_k moves to the boundary of its deviation range. The red dotted sphere centered at O_1 with a radius of $Rc(k)$ in Fig. 3(a) shows the communication range of node V_k at its deviation position at present time.

Step 2. When node V_k moves to two symmetrical positions of a deviation circle, there is an intersection area because the communication radius is greater than the deviation radius, as shown in Fig. 3(b). In Fig. 3(b), the black circle represents a deviation circle. The gray dotted spheres with a radius $Rc(k)$ show the 3D communication ranges of node V_k at the two symmetrical positions. The red areas represent the intersection areas between the two communication ranges.

Step 3. The intersection area can be obtained by calculating the communication and the deviation radii. As shown in Fig. 3(b), the minor and
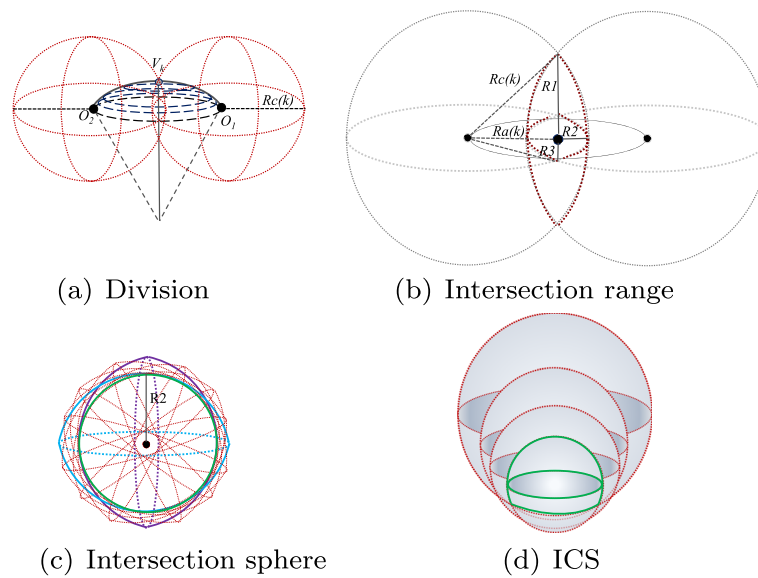
(a) Division

(b) Intersection range

(c) Intersection sphere

(d) ICS

Fig. 3 The calculation steps of ICS

major axis semidiameters of the intersection area can be obtained from the communication and current deviation radii. The major axis semidiameter $R1(k) = R3(k) = \sqrt{Rc(k)^2 - Ra(k)^{t2}}$, minor axis semidiameter $R2(k) = Rc(k) - Ra(k)^t$, and $\sqrt{Rc(k)^2 - Ra(k)^{t2}} > (Rc(k) - Ra(k)^t)$.

Step 4. As shown in Fig. 3(c), the purple area is the intersection area that described in the Fig. 3(b). As the node moves, it becomes the blue area in Fig. 3(c) when the intersection area rotates 180 degrees. As the intersection region rotates, the intersection of all possible communication areas on a deviation circle is a sphere with radius R2(k), as shown in Fig. 3(c). There is an intersection area on each deviation circle. The intersection of the intersecting areas on all deviation circles constitutes an inevitable communication space (ICS). Regardless of where the node is within its deviation range, AUV can communicate with the node granted it passes through the ICS.

For $\forall V_k \in V$, when the node moves from boundary position to initial position, $\sin \phi_k^t$ and $Ra(k)^t$ decrease, since $Ra(k)^t = l_k \sin \phi_k^t$. Because communication radius $Rc(k)$ is a fixed value, and the deviation radius $Ra(k)^t$ decreases as the offset angle decreases, *R1(k), R2(k)*, and *R3(k)* are all increased. The intersection area with radius R2(k) increases gradually as shown in Fig. 3(d). When $Ra(k)^t = Ra_m$ (i.e., $R2(k) = Rc(k) - Ra_m$), the intersection area is at the minimum, and when $Ra(k)^t = 0$ (i.e., $R2(k) = Rc(k)$), the intersection area is at the maximum. The ICS of node can be seen as the intersection of the maximum and minimum intersection area. The green area in Fig. 3(d) represents the ICS of node.

Hence, for $\forall V_k \in V$, the $ICS(V_k, Rc(k))$ can be calculated using the communication range and the deviation radius. The ICS of node satisfies the following conditions:

$$\begin{cases} (x - x_k^0)^2 + (y - y_k^0)^2 + (z - l_k)^2 \leq Rc^2 \\ (x - x_k^0)^2 + (y - y_k^0)^2 + (z - l_k \cos \theta)^2 \leq (Rc - Ra_m)^2 \end{cases} \quad (2)$$

where (x_k^0, y_k^0, l_k) is the initial position coordinate of node V_k, and $(x_k^0, y_k^0, l_k \cos \theta)$ is the center coordinate of the maximum deviation circle of node V_k.

Therefore, the ICS of a node can be calculated using the initial position, maximum offset angle, communication radius, and maximum deviation radius. And the size of ICS is mainly determined by the minimum value of *R2*, the minimum value of *R2* is $R2 = Rc - Ra_m = Rc - l_k \sin \theta$.

ICS-DDCA

Path planning procedure

According to the ICS obtained in previous section, this section combines ICS and path planning of AUV to reduce the time of data collection. Suppose AUV can move continuously in any direction and stop anywhere, and the area has no obstacles that hinder AUV movement. AUV dives underwater at regular intervals to collect relevant data sensed by the anchored nodes.

Most methods regard the path planning of AUV as a traveling salesman problem (TSP), which is a class of NP hard problems. AUV moves to the initial position of the nodes to collect data. If the node deviates from its initial position, its current position coordinates need
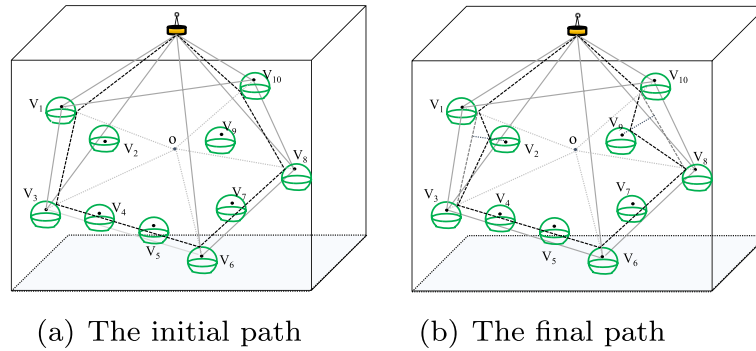
(a) The initial path   (b) The final path

Fig. 4 The process of ICS-DDCA

to be predicted using different prediction approaches. Then AUV moves toward the predicted position coordinates of node. The operations of location prediction and AUV movement are repeated until AUV successfully visits all nodes and collects the data. The uncertainty movement of nodes increases the difficulty of data collection, as well as the time of collection.

The focus of this study is to propose an ICS-based dynamic data collection algorithm (ICS-DDCA), in which AUV moves to ICS rather than the initial position of node to visit nodes and collect data. The travel time of AUV from node V_i to node V_j is $t(i,j) = \frac{d(p_i,p_j)}{v_m}$, where $d(p_i, p_j)$ is the travel distance of AUV, p_i is the point in $ICS(V_i, Rc(i))$, and v_m is the moving velocity of AUV. Suppose that AUV starts from the sink node. Then, the objective function that minimizes the data collection time can be formulated as:

$$Min(\sum_{i}^{N+1} \sum_{j}^{N+1} a_{ij} t(i,j))$$

$$s.t. \sum_{i \in V} a_{ij} = 1, \forall j \in \{1, \cdots, N+1\}, i \neq j$$

$$\sum_{j \in V} a_{ij} = 1, \forall i \in \{1, \cdots, N\}, i \neq j \qquad (3)$$

$$\sum_{i}^{N+1} \sum_{j}^{N+1} a_{ij} = N+1$$

$$a_{ij} = \{0, 1\}, \forall i, j \in V$$

If AUV moves from node V_i to V_j, then $a_{ij} = 1$, otherwise $a_{ij} = 0$. The first constraint indicates that AUV can only leave once for each node. $N + 1$ indicates that AUV eventually returns to the sink node and unloads the collected data. The second constraint means that AUV can only arrive once to each node. The third constraint indicates that all nodes must be visited. In contrast to the traditional methods that use the original position directly for the distance calculation, our proposed

method also needs to consider the uncertainty caused by node mobility when calculating the movement distance for AUV.

In order to plan the path of AUV, we must solve the problems of determination of target node and the determination of destination location coordinates on ICS of the target node. The target node is determined based on the 3D convex hull algorithm. After selecting the target node V_k, it is necessary to determine a point p_k in ICS as the destination location coordinates after AUV moves. The details of ICS-DDCA are as follows:

Step 1. The calculation of ICS. The ICS of each anchored node is calculated using Eq. (2). Then, the boundary information of ICS is determined.

Step 2. The selection of target node. Using the 3D convex hull algorithm, a maximum 3D convex polyhedron is determined by connecting the initial location coordinates of nodes to the sink node, as shown by gray solid line in Fig. 4(a).

Step 3. The center of the convex polyhedron is point *o*. The intersection of the line between the vertex and the center of convex polyhedron and the ICS of node is regarded as the target location point. These target location points are connected as the initial path, as indicated by black dotted line in Fig. 4(a).

Step 4. There are still some discrete anchored nodes in polyhedron. When the minimum distance between initial position of these nodes and the nearest initial path is less than communication radius, AUV can visit these node when passing through this path. Otherwise, the target location points of these nodes need additional calculation. The intersection of the shortest distance and ICS is regarded as the target location point of discrete sensor nodes, as indicated by black dotted line in Fig. 4(b).

Step 5. The total time of AUV visiting all nodes is calculated.

The process of data collection is described as Algorithm 1.

Input: V, θ, N, v_m, Rc, S
Output: T
1: **for** $V_k \in$ V **do**
2:    Calculate boundary location coordinates of nodes using Eq. (1)
3:    Calculate ICS of nodes using Eq. (2)
4: **end for**
5: Initialize f=0
6: Initialize T=0
7: Initialize $V^{'} = NULL$
8: Initialize $VS_p \leftarrow S$
9: The maximum 3D convex polyhedron CP_p is determined, and the set of nodes that make up the polyhedron is $V^{'}$. The vertices of the polyhedron form a visit sequence in a counter clockwise sequence, *VS*
10: The target location point of the nodes in *VS* is calculated, VS_p
11: **while** $f \leq N - |V^{'}|$ **do**
12:    **if** $\min\limits_{V_k \in V - V^{'}} d(V_k, CP_p) > Rc(k)$
13:       Calculate $p_k \in ICS(V_k, Rc(k))$
14:       $VS_p \leftarrow VS_p + p_k$
15:    **end if**
16: **end while**
17: $T = \sum_{k=1}^{|VS_p|-1} \left\{ \frac{d(VS_p(k), VS_p(k+1))}{v_m} \right\}$

Algorithm 1 Data Collection Algorithm ICS-DDCA-This algorithm operates as follows. First, according to the communication radius and the maximum offset angle θ, the boundary location coordinates, where the node moves to the boundary of its deviation range, are computed using Eq. (1) for each node in V. The ICS of a node is calculated using Eq. (2) (Lines 1 to 4). The initialization parameters and the maximum 3D convex polyhedron are determined by connecting the initial location coordinates of nodes to the sink node (Lines 5 to 9). Then, according to the ICS of nodes, target location points are calculated, and the visit sequence is determined (Lines 10). By calculating the distance between discrete nodes and convex polyhedron, we can determine whether the discrete nodes can be visited. If the distance is greater than communication radius, the target location point on ICS needs to be calculated (Lines 11 to 16). When all nodes are visited, the time of data collection T is returned.

Analysis of ICS-DDCA
The advantage of ICS
Let's first analyze the advantages of ICS computing for data collection. In the case of communication radius is large enough, in order to ensure that AUV can communicate with node, it moves to the initial position of
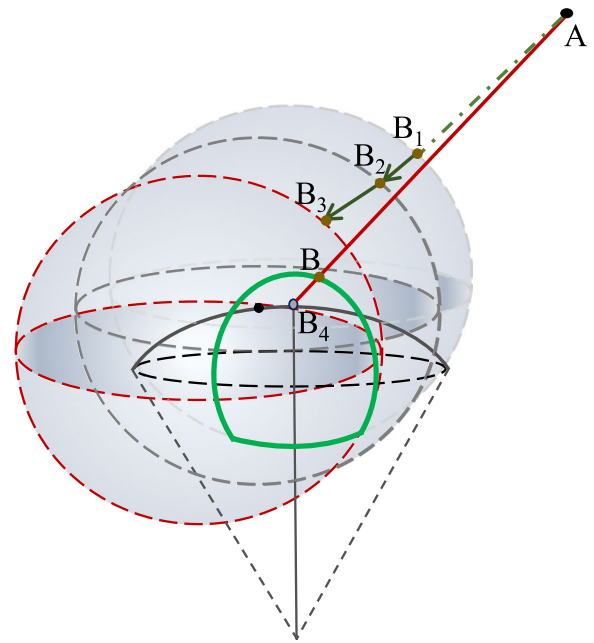

Fig. 5 Comparison of calculating distance

node to collect the data. As shown in the Fig. 5, AUV moves from point A to the initial position B_4 of node to collect data, and the moving distance is $|AB_4|$. For ICS-DDCA, the effect of data collection using ICS of node is the same as that using initial position. However, if ICS of node is used, the moving distance of AUV is $|AB|$, and $|AB| < |AB_4|$. That is, using ICS of node can reduce the unnecessary path of AUV moving from region boundary of ICS to initial position of node, which helps to shorten the path length of AUV and time of data collection.

If AUV communicates with a node based on the communication radius, that is, AUV moves to the edge of the communication area to communicate with the node, AUV needs to adjust the movement trajectory according to the position of node. Some localization or prediction schemes are used to determine the location of nodes. The trajectory of AUV moving with node is shown in Fig. 5. The moving distance of AUV based on the position of node is $|AB_1|$. For effective data collection, the trajectories of AUV moving with the node are $|B_1B_2|$ and $|B_2B_3|$. Owing to the limitations of cost, energy, and environment, the locations of nodes are inaccurate. In other words, the movement of node in its deviation range increases the path length of AUV and the time of data collection. Moreover, positioning and prediction algorithm increase the cost of network. Compared with using communication radius, using ICS can avoid some needless moving paths of AUV due to AUV moves with node.

Guang *et al. Journal of Cloud Computing*   (2023) 12:46

Page 9 of 14

Analysis of complexity

The time complexity of PNCS-GHA is $O(N^2)$. For EEDA, the time complexity of constructing a optimal rigid graph in a subarea is $O(N^3)$. Thus, the complexity of constructing rigid graphs in M subareas is $O(M \cdot N^3)$. The complexity of routing algorithm in a subarea is $O(N)$. Therefore, the complexity of EEDA is $O(M \cdot N^3)$. The time complexity of ICS-DDCA is related to the number of nodes. The time complexity for calculating ICS of nodes is $O(N)$. According to algorithm 1, the complexity of constructing a convex polyhedron is $O(NlogN)$. The time complexity of adding discrete nodes to the visit sequence composed of a 3D convex polyhedron is $O(N - M)$, where M is the number of nodes that make up the polyhedron. As a result, the time complexity of ICS-DDCA is $O(N) + O(NlogN) + O(N - M) = O(NlogN)$. Therefore, the complexity of the proposed scheme is smaller than those of the EEDAc and PNCS-GHA. The performance advantage of ICS-DDCA is shown by the simulation results in next section.

Simulation evaluation

ICS-DDCA is evaluated by observing the performance variation when adopting different parameters and by comparing ICS-DDCA to EEDA, PNCS-GHA. For EEDA, AUV selects the next cluster to be visited based on the distance. AUV moves to the communication range of cluster-head node to collect data. If cluster-head node moves out of the communication range of initial position, the path of AUV needs to be adjusted according to the node position to complete the data collection. PNCS-GHA is a nearest neighbor heuristic trajectory planning algorithm, in which AUV traverses a probabilistic neighborhood covering set for data collection. Similarly, the path of AUV needs to be adjusted again when node moves out of the communication range of initial position. EEDA-ICS is the improved algorithm of EEDA that takes into account the ICS of node.

ICS-DDCA is implemented in MATLAB, and the result is the average of 10 repetitive simulation results. N anchored sensor nodes are randomly distributed in an underwater convex space. Every node has the same maximum offset angle.

The offset angle is determined by the velocity and direction of water flow that lashes the node. The relationship between velocity of the water flow and offset angle can be analyzed through the force balance of node [34]. According to the result of [34], it can be calculated as

$$\phi_k^t = \arctan \xi \overrightarrow{u_k(t)}^2, \qquad (4)$$

where ξ is a constant environmental parameter value, and $\overrightarrow{u_k(t)}$ is the velocity at which the water flow lashes node

V_k at time t. In the multi-layer current model, the current velocity is related to depth. The nearer a layer is to the water surface, the greater the water flow rate is. The water velocity is u.

It can be observed from Eq. (4) that offset angle ϕ_k^t of node V_k in time t is related to the square of velocity $\overrightarrow{u_k(t)}^2$. Furthermore, when the velocity reaches its maximum value, the offset angle can also obtain its maximum value. In other words, the offset angle can be obtained when the velocity and direction of the current are given. In multi-layer current model, the velocity and direction of water flow are constant at a certain depth. In other words, the velocity of water flow affects the offset angle and the movement of nodes. The parameters are shown in Table 2.

The effect of number of nodes

The data collection time with respect to varying number of nodes using EEDA, PNCS-GHA, EEDA-ICS, and ICS-DDCA are compared. Figure 6 illustrates the data collection time with $Rc = 200m$ and $v_m = 1m/s$. From Fig. 6, it is observed that the data collection time of ICS-DDCA is less than that of the other algorithms. Because the ICS-DDCA proposed in this study states that AUV moves directly to ICS to collect data, AUV does not need to move according to the node deviation. For EEDA-ICS, AUV moves directly to ICS to collect data as well. Therefore, it takes less time than EEDA. For EEDA and PNCS-GHA, AUV needs to move according to the node deviation. Therefore, they take more time than ICS-DDCA.

The effect of communication radius

Figure 7 shows that the communication radius of sensor nodes has a significant influence on data collection time. With an increase in the communication radius, the ICS becomes larger, so it takes less time for AUV to collect data from ICS than from initial position. Therefore, ICS-DDCA effectively reduces the time required

Table 2 The basic simulation parameters

Parameter	Description	Value
N	Number of sensor nodes	5-30
$L \times W \times H$	Deployment space	$10^3 \times 10^3 \times 10^3 m$
Rc	Communication radius	50-500m
θ	Maximum offset angle	$\pi/18$
u	Water velocity	0.5-2m/s
v_m	Speed of AUV	0.5-5 m/s
m	Number of layers	5

Guang *et al. Journal of Cloud Computing* (2023) 12:46
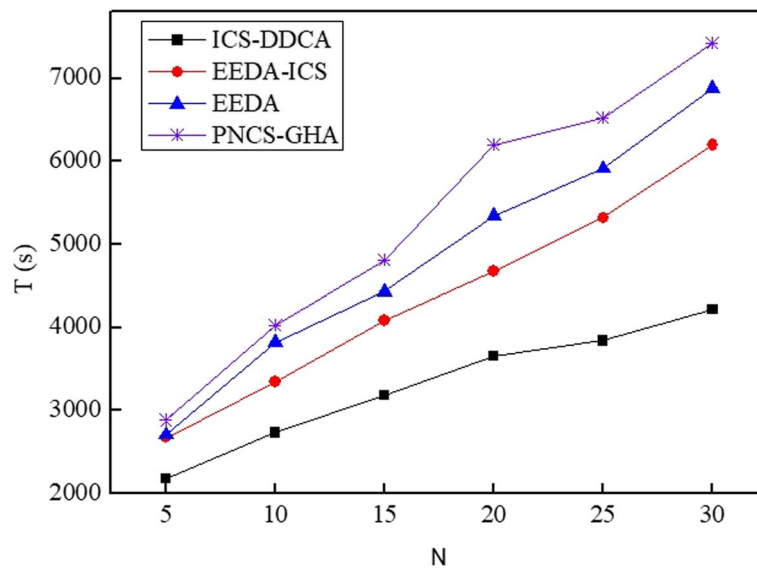
Page 10 of 14

Fig. 6 Data collection time with different *N*

for data collection via the ICS construction. With an increase in communication radius, the advantages of ICS-DDCA are becoming increasingly obvious. When communication radius is sufficiently large, AUV can successfully collect data as long as it passes the initial location of node. Therefore, when $N = 5$ and $v_m = 1m/s$, the data collection time of PNCS-GHA remains unchanged after $Rc = 250m$. Compared to EEDA and PNCS-GHA, ICS-DDCA reduces the time required for data collection by 26.7% and 33.84%, respectively, when $Rc = 250m$. When communication radius is large enough, the time

of ICS-DDCA cannot be infinitely reduced, it tends to a certain range. For EEDA-ICS, AUV moves directly to ICS to collect data, and AUV does not need to move with node. Therefore, it takes less time than the EEDA. However, it selects the node closest to AUV as the next visit node. It tends to be trapped in local optima. Therefore, it takes more time than the ICS-DDCA.

The effect of the speed of AUV

The speed of AUV has a significant influence on the data collection time, as shown in Fig. 8. Figure 8(a)
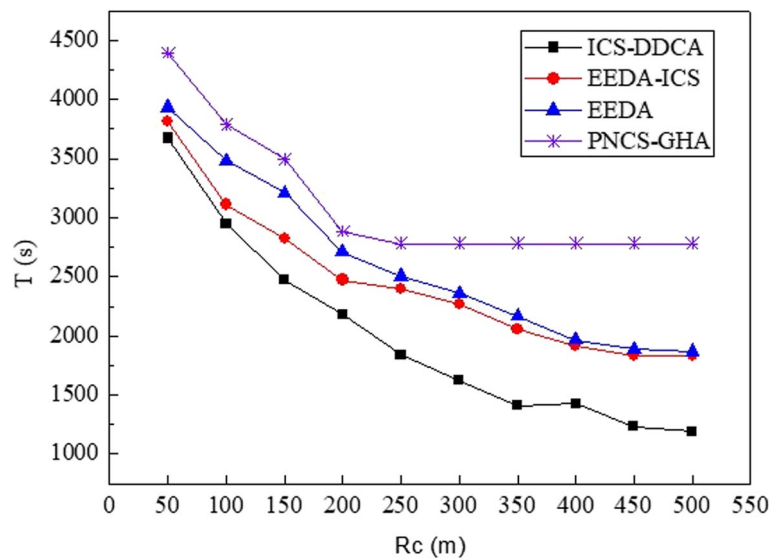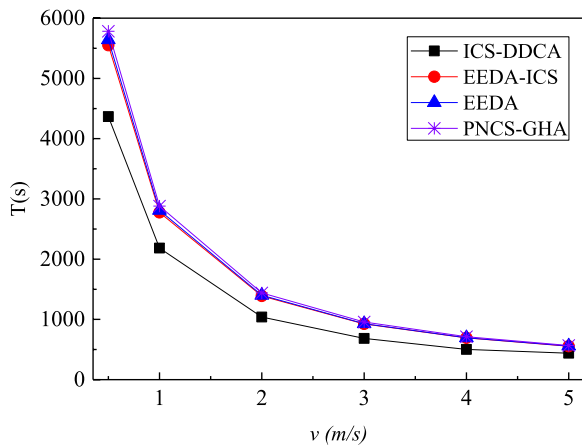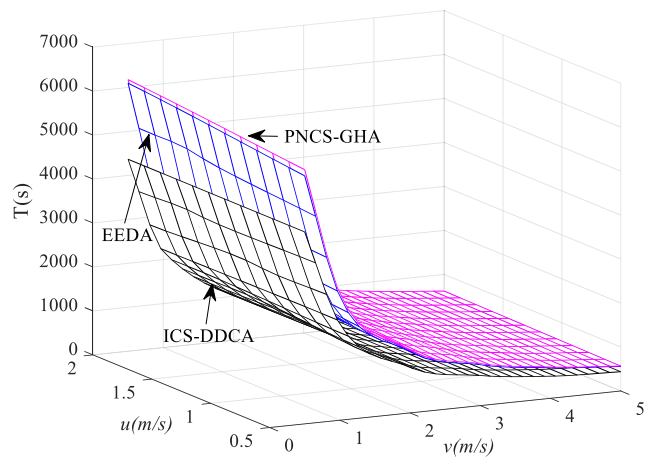

Fig. 7 Data collection time with different *Rc*

(a) Influence of v_m (b) Influence of u and v_m

Fig. 8 The effect of the speed of AUV

shows a comparison of the data collection times of EEDA, PNCS-GHA, EEDA-ICS, and ICS-DDCA with respect to different speed settings of AUV, where $N = 5$ and $Rc = 200m$. In Fig. 8(a), when the speed of AUV is very small, it requires more time to chase the moving sensor nodes. For EEDA and PNCS-GHA, it takes a longer time to complete data collection. However, when the speed of AUV is greater, the collection time is reduced. When the speed of AUV is greater, it can catch up with the sensor nodes to complete data collection before the node moves too far. According to Fig. 8(a), we can conclude that the time of ICS-DDCA is less than EEDA, PNCS-GHA, and EEDA-ICS regardless of the change in AUV speed. This is because AUV in ICS-DDCA passes through the ICS of node to collect data. When the speed of AUV is greater, the results of EEDA and EEDA-ICS are almost the same. In the follow-up analysis, ICS-DDCA is mainly compared with EEDA and PNCS-GHA.

The mobility of anchored nodes has a significant influence on data collection time. In Fig. 8(b), Z-axis represents the time taken by AUV to complete data collection, X-axis represents the speed of AUV, and Y-axis represents the water velocity. According to physical oceanography, the water velocity is usually 1 m/s to 2 m/s on average. The water velocities of 1m/s and 2m/s are recorded as the general velocity and faster velocity, respectively. The water velocity cannot be zero in the actual situation. In this paper, the flow velocity of 0.5m/s is considered close to static [26]. When the water flows slowly, nodes move slightly (nodes can be regarded as stay at the initial position), the time required for data collection will be reduced

with the increase of the speed of AUV. When the speed of AUV is large enough, the time of ICS-DDCA is close to that of EEDA and PNCS-GHA. However, when AUV is slow, even if the nodes move slightly, AUV still requires more time to chase the moving sensor nodes. Thus, it takes more time to complete data collection. Compared to EEDA and PNCS-GHA, the time required for data collection of ICS-DDCA is significantly shorter.

The effect of node movement

The influence of node mobility and communication radius on time was observed and analyzed in this simulation. Two observations can be seen in Fig. 9. When u is fixed, an increase in Rc results in a reduction in collection time. When communication radius is sufficiently large, the data collection time of PNCS-GHA remains unchanged, while the data collection time of EEDA and ICS-DDCA tends to a certain range. The time of EEDA and PNCS-GHA is greater than that of ICS-DDCA. The time of PNCS-GHA is also greater than that of the EEDA. If communication radius is sufficiently large, AUV can successfully collect data when it moves to initial position of node. For EEDA, AUV moves to communication range of the node to collect data. Therefore, the time of EEDA is less than that of PNCS-GHA. When Rc is fixed, the collection time increases as u increases. If nodes move frequently, AUV requires more time to chase the moving sensor nodes. For ICS-DDCA, when Rc is sufficiently large, the offset movement of nodes does not lead to a change in data collection time. No matter how the nodes move, as long as the ICS is formed, AUV can pass through ICS to collect data. Therefore, the value of u has
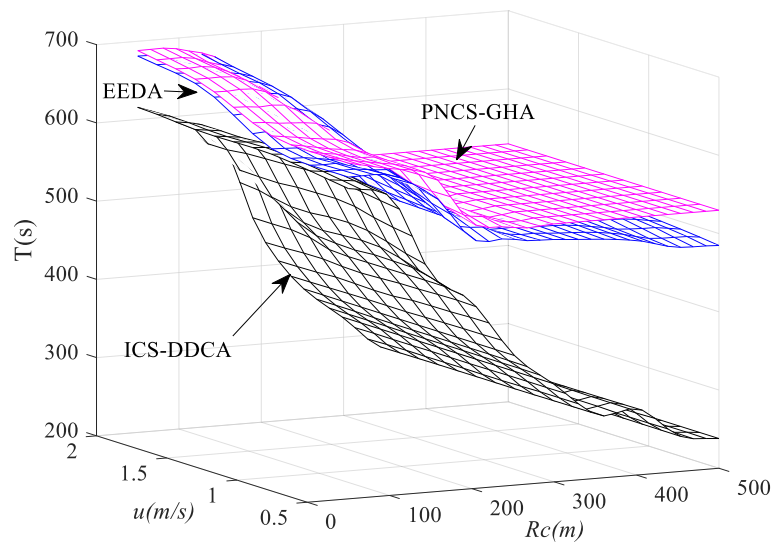
Fig. 9 Influence of node mobility and radius

an inconspicuous effect on the collection time when Rc is sufficiently large.

The effect of length of anchor rope
For multi-layer current model, the layer with greatest depth has the smallest current velocity. The depth of node is determined by the length of anchor rope. The nodes close to the water surface with a longer anchor rope are greatly affected by the flow. Thus, these nodes move more frequently. In addition, for $\forall V_k \in V$, the maximum deviation radius of V_k is defined as $Ra_m(k) = l_k \sin\theta$, and $Ra_m(k) < Rc(k)$. When the maximum offset angle θ is fixed, the maximum deviation radius increases as l_k increases. According to the previous analysis, the major and minor axis semi-diameters of the intersection area on a deviation circle are $R1(k) = R3(k) = \sqrt{Rc(k)^2 - Ra(k)^{t2}}$, and $R2(k) = Rc(k) - Ra(k)^t$, respectively. Because communication radius $Rc(k)$ is a fixed value, and the deviation radius $Ra(k)^t$ increases as l_k increases, while R1(k), R2(k), and R3(k) all decrease. Thus, the ICS of node V_k is small. The nodes with longer anchor ropes have greater deviation ranges and smaller ICS. For $\forall V_k \in V$, when communication radius $Rc(k) = 200m$ and the maximum offset angle $\theta = \pi/18$, the length of anchor rope can be calculated as $l_k < Rc(k)/\sin\theta$.

Figure 10 illustrates the influence of the length of anchor rope with $Rc(k) = 200m$, $\theta = \pi/18$, $v_m = 1m/s$, and $N = 5$. When u is fixed, an increase in l_k results in a reduction in collection time. As l_k becomes longer, the node is closer to the sink node located on the water surface, and the time AUV takes to collect data becomes smaller. However, ICS of the node decreases

as l_k increases. Therefore, the time taken by AUV to collect data becomes dynamically smaller. The times of EEDA and PNCS-GHA are greater than that of ICS-DDCA. For ICS-DDCA, the offset movement of nodes does not lead to a change in data collection time when $Rc(k) = 200m$. AUV collects data via the ICS. For EEDA and PNCS-GHA, when l_k is fixed, the collection time increases as u increases. Therefore, regardless of the length of anchor rope, as long as the ICS can be formed, ICS-DDCA requires less time to collect data.

Therefore, ICS-DDCA effectively shortens the time of data collection in 3D UIoT. Compared to PPM-LUWSN proposed by Zhou et al., we propose the concept of ICS and extend the ICS to a 3D underwater environment. In dynamic underwater sensor networks, it is important to consider both the ICS and path planning of AUV. This algorithm, which considers the joint problem of ICS and path planning, is also suitable for other 3D scenes.

Conclusion
To solve the dynamic data collection problem of node location uncertainty in complex marine environments, we propose an ICS-based dynamic data collection algorithm (ICS-DDCA). First, the concept of an inevitable communication space (ICS) is proposed. The ICS is obtained by analyzing the deviation range and communication radius of anchored sensor nodes. Then, the problems of ICS and path planning are considered jointly to improve the performance of data collection algorithms and shorten the data collection time. Compared to previous algorithms, ICS-DDCA extends the concept of ICS to a 3D underwater environment and improves the performance of
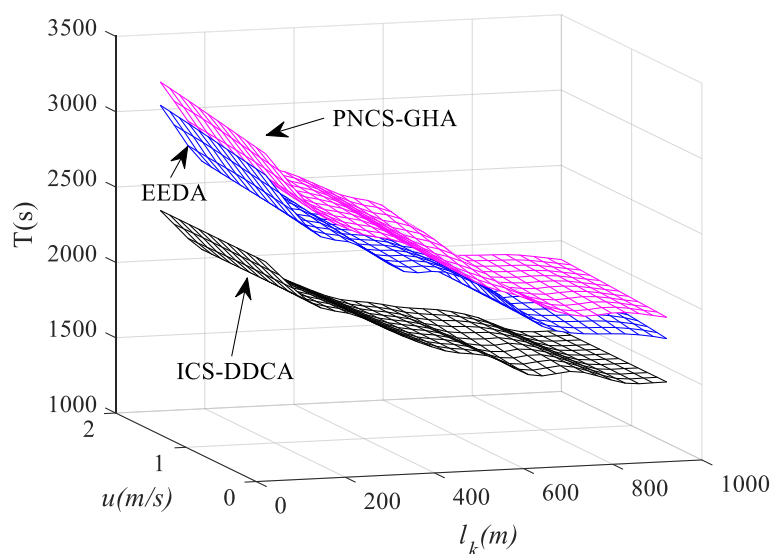
Fig. 10 The effect of length of anchor rope

underwater data collection algorithms. The simulation results show that ICS-DDCA shortens the time of data collection through constructing ICS. Compared to EEDA, PNCS-GHA, and EEDA-ICS, ICS-DDCA reduces the time required for data collection. Compared to EEDA, EEDA-ICS reduces the time required for data collection. AUV does not need to be adjusted when nodes deviate from their initial positions. Thus, the ICS concept can be combined with other algorithms to further improve the performance of the algorithms.

In the future work, the proposed algorithm can be applied to other application scenarios, such as, target detection, navigation and obstacle avoidance, hierarchical data collection, and multi-objective path planning. The concept of ICS can also be introduced into other dynamic path planning algorithms of AUV to further shorten the path length of AUV. And in the process of data collection, the influence of motion status and velocity of AUV are not considered. In the future work, we will analyze the impact of motion status and velocity of AUV on data collection. In addition, the size of ICS can be changed by adjusting the power of nodes to reduce energy consumption and ensure communication. And this will be the focus of our future work. Besides, the data collection of heterogeneous nodes is also a research focus of our future work.

Abbreviations

IoT	Internet of things
UIoT	Underwater internet of things
UWSNs	Underwater wireless sensor networks
AUV	Autonomous underwater vehicles
ICS	Inevitable communication space
ICS-DDCA	ICS-based dynamic data collection algorithm

Authors' contributions
Xiaoyun Guang, Chunfeng Liu, Wenyu Qu, Zhao Zhao designed the study and write the paper. Xiaoyun Guang performed the simulations. All authors reviewed and edited the manuscript. All authors read and approved the final manuscript.

Authors' information
Xiaoyun Guang is a Ph.D. candidate in the College of Intelligence and Computing, Tianjin University, China. Her research interests include complex network and underwater sensor networks. Email: guangxiaoyun@tju.edu.cn. Chunfeng Liu is an associate professor at the College of Intelligence and Computing, Tianjin University, China. Her research interests include wireless network, traffic modeling, protocol design, performance evaluation and QoS, and truthful computing in non-cooperative wireless networks. Email: cfliu@tju.edu.cn.
Wenyu Qu is a professor at the College of Intelligence and Computing, Tianjin University, China. Her research interests include cloud computing, computer networks, and information retrieval. Email: wenyu.qu@tju.edu.cn. Zhao Zhao is a Ph.D. candidate in the College of Intelligence and Computing, Tianjin University, China. His research interests include underwater sensor networks. Email: zhaoz526@foxmail.com.

Availability of data and materials
The data used to support the findings of this work is available from the corresponding author upon request.

Declarations

Competing interests
The authors declare that they have no competing interests.

Guang *et al. Journal of Cloud Computing* (2023) 12:46

Page 14 of 14

References

1. Qiu T, Chen N, Li K, Atiquzzaman M, Zhao W (2018) How can heterogeneous internet of things build our future: a survey. IEEE Commun Surv Tutor 20(3):2011–2017
2. Xiao T, Chen L, Sha C, Sun L, Wang R, Liu A, Ahmed F (2018) Noise tolerant localization for sensor networks. IEEE/ACM Trans Networking 26(4):1701–1714
3. Yu K, Yu J, Cheng X, Yu D, Dong A (2021) Efficient link scheduling solutions for the internet of things under rayleigh fading. IEEE/ACM Trans Networking 29(6):2508–2521
4. Yu K, Wang Y, Yu J, Yu D, Cheng X, Shan Z (2019) Localized and distributed link scheduling algorithms in iot under rayleigh fading. Comput Netw 151(14):232–244
5. Wang T, Zhang G, Alam BZ, Liu A, Jia W, Xie M (2018) A novel trust mechanism based on fog computing in sensor-cloud system. Futur Gener Comput Syst 109:573–582
6. Qiu T, Zhao Z, Zhang T, Chen C, Chen C (2020) Underwater internet of things in smart ocean: System architecture and open issues. IEEE Trans Ind Informat 16(99):1
7. Mohsan S, Mazinani A, Othman N, Amjad H (2022) Towards the internet of underwater things: A comprehensive survey. Earth Sci Inform 15:735–764
8. Mary D, Ko E, Kim S, Yum S, Shin S, Park S (2021) A systematic review on recent trends, challenges, privacy and security issues of underwater internet of things. Sensors 21(24):8262
9. Coutinho RWL, Boukerche A, Vieira LFM, Loureiro A (2016) A novel centrality metric for topology control in underwater sensor networks. MSWiM'16: Proceedings of the 19th ACM International Conference on Modeling, Analysis and Simulation of Wireless and Mobile Systems, New York, pp 205–212
10. Cai S, Zhu Y, Wang T, Xu G, Liu A (2019) Data collection in underwater sensor networks based on mobile edge computing. IEEE Access 7:65357–65367
11. Zhao Z, Qu W, Liu C, Qiu T, Guang X (2019) A novel self-organizing routing algorithm for underwater internet of things. 2019 IEEE 23rd International Conference on Computer Supported Cooperative Work in Design (CSCWD), Porto, pp 470-475. https://doi.org/10.1109/CSCWD.2019.8791882
12. Hollinger GA (2012) Underwater data collection using robotic sensor networks. IEEE J Sel Areas Commun 30(5):899–911
13. Qiu T, Li B, Qu W, Ahmed E, Xin W (2019) Tosg: A topology optimization scheme with global small world for industrial heterogeneous internet of things. IEEE Trans Ind Inform 15(6):3174–3184
14. Ghoreyshi SM, Shahrabi A, Boutaleb T (2017) Void-handling techniques for routing protocols in underwater sensor networks: Survey and challenges. IEEE Commun Surv Tutor 19(2):800–827
15. Boukerche A, Coutinho RWL, Loureiro AAF, Vieira LFM (2018) Underwater wireless sensor networks: A new challenge for topology control-based systems. ACM Comput Surv 51(1):19.1–19.36
16. Duan R, Du J, Jiang C, Ren Y (2020) Value based hierarchical information collection for auv enabled internet of underwater things. IEEE Internet Things J PP(99):1
17. Chen YS, Lin YW (2013) Mobicast routing protocol for underwater sensor networks. IEEE Sensors J 13(2):737–749
18. Gjanci P, Petrioli C, Basagni S, Phillips C, Boloni L, Turgut D (2018) Path finding for maximum value of information in multi-modal underwater wireless sensor networks. IEEE Trans Mob Comput 17(2):404–418
19. Yan H, Shi ZJ, Cui JH (2008) DBR: Depth-based routing for underwater sensor networks. NETWORKING 2008 Ad Hoc and Sensor Networks, Wireless Networks, Next Generation Internet. NETWORKING 2008. Lecture Notes in Computer Science, Springer, Berlin, 4982:72-86. https://doi.org/10.1007/978-3-540-79549-0_7
20. Rahman MA, Lee Y, Koo I (2017) Eecor: An energy-efficient co-operative opportunistic routing p rotocol f or underwater acoustic sensor networks. IEEE Access 5:14119–14132
21. Dong M, Ota K, Liu A (2017) Rmer: Reliable and energy-efficient data collection for large-scale wireless sensor networks. IEEE Internet Things J 3(4):511–519
22. Yuan Y, Liang C, Kaneko M, Chen X, Hogrefe D (2019) Topology control for energy-efficient localization in mobile underwater sensor networks using stackelberg game. IEEE Trans Vehicular Technol, 68(2):1487-1500
23. Han G, Li S, Jiang J, Zhu C, Zhang W (2017) Data collection algorithms based on probabilistic neighborhood for underwater acoustic sensor networks. Sensors 17(2):316
24. Yan J, Yang X, Luo X, Chen C (2018) Energy-efficient data collection over AUV-assisted underwater acoustic sensor network. IEEE Syst J 12(4):3519-3530
25. Zhou J, Yang J, Xiao F, Yan X, Liu L (2019) Path planning method based on the location uncertainty of water surface nodes in underwater sensor network. 2019 IEEE 25th International Conference on Parallel and Distributed Systems (ICPADS), Tianjin, pp 711-716
26. Han G, Shen S, Song H, Yang T, Zhang W (2018) A stratification-based data collection scheme in un-derwater acoustic sensor networks. IEEE Trans Veh Technol 67(11):10671–10682
27. Gao X, Chen Z, Wu F, Chen G (2017) Energy efficient algorithms for k-sink minimum movement target coverage problem in mobile sensor network. IEEE/ACM Trans Networking PP(6):1–12
28. Khan M, Ahmed SH, Jembre YZ, Kim D (2019) An energy-efficient data collection protocol with auv path planning in the internet of underwater things. J Netw Comput Appl 135:20–31
29. Cheng CF, Li LH (2016) Data gathering problem with the data importance consideration in underwater wireless sensor networks. J Netw Comput Appl 78:300–312
30. Liu L, Wang R, Xiao F (2012) Topology control algorithm for underwater wireless sensor networks using gps-free mobile sensor nodes. J Netw Comput Appl 35(6):1953–1963
31. Liu L, Zhang N, Liu Y (2015) Topology control models and solutions for signal irregularity in mobile underwater wireless sensor networks. J Netw Comput Appl 51:68–90
32. Pompili D, Melodia T, Akyildiz IF (2006) Deployment analysis in underwater acoustic wireless sensor networks. WUWNet '06: Proceedings of the 1st International Workshop on Underwater Networks, New York, pp 48–55
33. Halkin D, Rossby T (2010) The structure and transport of the gulf stream at 73°w. J Phys Oceanogr 15(11):1439–1452
34. Liu C, Zhao Z, Qu W, Qiu T, Sangaiah AK (2019) A distributed node deployment algorithm for underwater wireless sensor networks based on virtual forces. J Syst Archit 97:9–19

Publisher's Note

Springer Nature remains neutral with regard to jurisdictional claims in published maps and institutional affiliations.